06 Oct 1971

Boundary Pressure Fluctuations Due to Macroturbulence in Hydraulic Jumps

F. R. Schiebe

C. E. Bowers

BOUNDARY PRESSURE FLUCTUATIONS DUE TO MACROTURBULENCE IN HYDRAULIC JUMPS

Frank R. Schiebe
St. Anthony Falls Hydraulic Laboratory
University of Minnesota
Minneapolis, Minnesota

C. Edward Bowers
Department of Civil and Mineral Engineering
University of Minnesota
Minneapolis, Minnesota

ABSTRACT

Data concerning the statistical properties of pressure fluctuations on the containment structure associated with the hydraulic jump have been studied at the St. Anthony Falls Hydraulic Laboratory. The incident Froude numbers were investigated through the practical range from 4 to 9. The mean square of the fluctuating pressure, the mean pressure, and the power spectrum were determined as a function of position under the jump. In addition, mean and rms turbulent velocity profiles and entrained air concentration profiles throughout the jump volume were determined.

The principal tests were performed in a channel 20 inches wide and 3 feet deep. Other tests at a larger scale were performed in a flume 9 feet wide and 6 feet deep to assist in an evaluation of the scaling properties of the various statistical parameters. The data indicate that the rapid rate of energy dissipation near the toe of the jump leads to a maximum rms fluctuation pressure on the bed of about 5 per cent of the incoming velocity head. The location of the maximum pressure fluctuation is approximately midway under the roller of the jump.

INTRODUCTION

The hydraulic jump is an economically and physically important phenomenon which has been used extensively to dissipate energy in connection with control structures on rivers. The energy is dissipated in a fairly short length of river by the creation of high-level turbulence in a high-shear zone in the jump. As a consequence of the turbulence, a high degree of mixing takes place and high fluctuating pressures are imposed on the boundaries of the channel.

It has been the usual engineering practice to conduct a model study to establish the optimum hydraulic design of a control structure. The performance of the prototype structure is predicted by the model study. Only in the last decade and a half has any attention been paid to the fluctuating components of the pressures imposed on the model structures. The neglect of these components can lead and has led to catastrophic structural failures. From a design standpoint the peak loads must be known as well as the range of frequencies in which the fluctuating pressure energy is concentrated. The minimum pressure possible must be known for cavitation considerations.

In this study an attempt has been made to experimentally establish the stochastic nature of the pressure fluctuations on the flat, horizontal bed under a hydraulic jump and the flow characteristics within the jump which produce and otherwise influence them.

EXPERIMENTAL

The energy dissipated in the hydraulic jump can be determined in terms of the conjugate upstream and downstream depths by solving the elementary momentum, energy, and continuity equations. In a somewhat more sophisticated analysis Rouse, et al.[1] have provided details of the process by which energy is extracted from the mean flow and transferred to the turbulence. The turbulent energy is then ultimately transformed into heat.

It has been shown[2] that the mechanisms which produce the pressure fluctuations consist of nine turbulence-mean shear interaction terms and nine more turbulence-turbulence interaction terms. In dealing with the smooth boundary layer case all but the single component,

$$\frac{\partial \overline{u_1}}{\partial x_2} \frac{\partial u'_2}{\partial x_1} ,$$

where $\frac{\partial \overline{u_1}}{\partial x_2}$ = longitudinal normal velocity gradient and $\frac{\partial u'_2}{\partial x_1}$ = vertical turbulence gradient in the longitudinal direction, have usually been neglected in the literature.

In the case of the two-dimensional hydraulic jump, a separated type of jet flow, it is not at all obvious that any of the terms, except possibly a few that contain lateral mean components of flow or lateral rates of change, can be neglected.

The major portion of this experimental investigation was carried out in the glass-sided laboratory flume shown in Figure 1, which is 20 inches wide, 36 inches deep, and 40 feet long. The channel is equipped with adjustable control gates and supplied with water from the Mississippi River through an independent metering weir section downstream. The flume was modified by the installation of a false bed to facilitate the mounting of flush-mounted strain element pressure transducers.

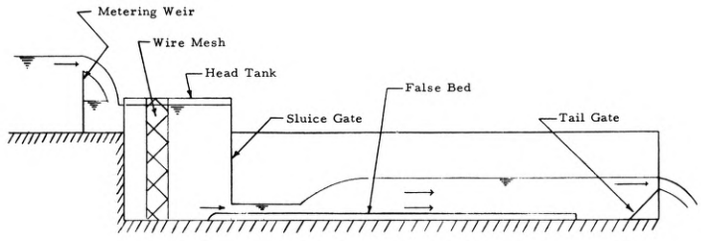

Figure 1. Schematic of the 20 inch Channel

In order to investigate the effects of scale, experimental tests were performed in the 9-foot-wide channel shown in Figure 2 with a maximum discharge capacity of 300 cfs. Tail and sluice gates and a head loss baffle were used to adjust the flow in the larger channel.

A number of difficulties are inherent in making measurements within the jump. A hydraulic jump is characterized by a developing flow region which exhibits large velocity gradients, a flow reversal in a portion of the region of interest, high concentrations of entrained bubbles producing a two-phase stratified situation, and very high turbulence levels.

The gas bubble concentrations were measured with a conductivity probe which was especially designed and calibrated for measurements in air-entrained flows.[3] The instrument consists of a probe, shown schematically in Figure 3, and an electronic circuit and is based fundamentally on measurement of the electrical resistance of fluid between the pair of electrodes which make up the probe. The probe was calibrated in the range of operation anticipated for the present study. The method used in this calibration was simply mixing independently measured flows of air and water and measuring the resulting fluid, adjusted to be in the bubbly regime, in a vertical pipe with the electronic probe. With proper calibration, the instrument reads out directly

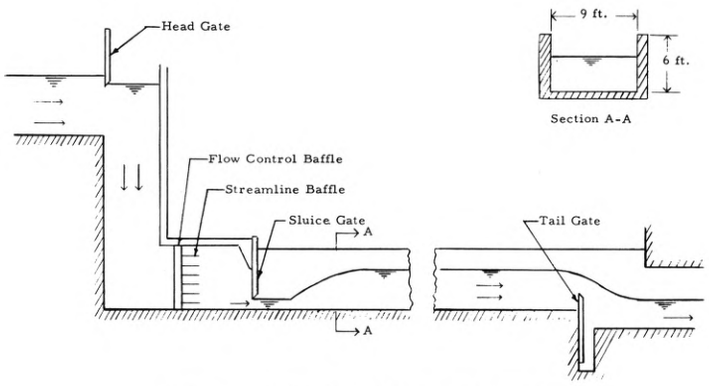

Figure 2. Scheme of the 9 Foot Test Channel

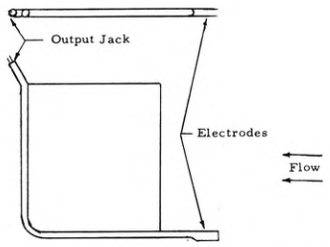

Figure 3. Scheme of Air Entrainment Probe

the percentage of water in the small fluid volume between the electrodes. It is estimated that these measurements are accurate to ± 5.0 per cent. The mean velocities were obtained using a total head tube with a flushing system to purge the gas bubbles from the line.

A transducer-coupled impact tube was used to measure the turbulent or fluctuating velocity component. This probe, shown in Figure 4, utilizes a pressure transducer in combination with a short impact tube, producing an electric signal which can be interpreted to represent the fluctuating velocity.

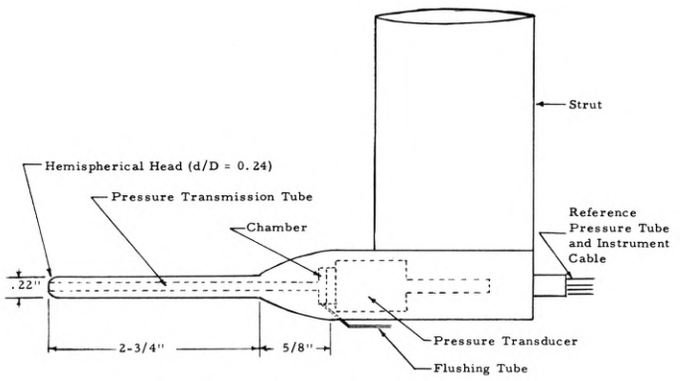

Figure 4. Turbulence Probe

The use of such probes has been *reported in the literature.*[4] A good deal of the work on this type of probe has utilized transducer elements of the piezo-electric type. These elements have definite limitations in that their response diminishes at low frequencies and disappears under a pure static load.

Since the frequencies of main interest in the present study are of the order of 1 or 2 Hz, it was determined that transducing units which employ strain elements in a bridge configuration should be used. This use effectively removed the low frequency limitations, since these units have a static response. The frequency bandwidth is determined by those factors which govern the natural frequency of the tube and chamber.

A modified flushing system was also used with this tube and the entire system was checked for frequency response. The system responded flat from D.C. to well over 100 Hz, which was more than adequate for the macroturbulent quantities of interest in the study.

In analyzing the response of such an instrument to an unsteady flow, the governing Bernoulli equation can be written:

$$\frac{1}{2}\rho u^2 - \rho \frac{\partial \phi}{\partial t} + p = F(t) \tag{1}$$

In an approximate analysis it can be assumed that the form of the velocity potential is not significantly different from that of a half-body derived by employing a point source in a uniform velocity field. If the geometry of such a body is held fixed in a uniform, but fluctuating velocity field, the source strength must be a function of time and be related to the velocity.

The velocity potential can then be written in terms of the body geometry and the velocity decomposed by the Reynolds substitutions. If x_s is the distance between the point source and the stagnation point, on the stagnation streamline:

$$\frac{\partial \phi}{\partial t} = \left(\frac{x_s^2}{x} + x \right) \frac{\partial u'}{\partial t} \tag{2}$$

Since our interest is in the turbulence at the stagnation point, as if the probe were not there, $x = x_s = R/2$ or half the body radius.

This pressure signal is converted to an electrical signal by the transducer. The electrical signal is then transmitted to a carrier amplifier recorder unit (Sanborn Mo. 350-1100B) where the signal can be recorded as a function of time. This amplifier also functions as a signal conditioner. A demodulated signal representing the pressure is available at an output jack. The signal can be averaged by switching in an averaging circuit and a D.C. component can be added or subtracted from the signal by an average position control. On the stagnation streamline, the total pressure sensed by the probe is:

$$\overline{p_T} + p_T' = \frac{1}{2}\rho \overline{u_1}^2 + \rho \bar{u}_1 u_1' + \frac{1}{2}\rho u_1'^2 + \bar{p} + p' - R \frac{\partial u_1'}{\partial t} \tag{3}$$

Taking the time average and subtracting from the above equation yields:

$$p_T' = \rho \bar{u}_1 u_1' + \frac{1}{2}\rho u_1'^2 - \frac{1}{2}\rho \overline{u_1'^2} + p' - R \frac{\partial u_1'}{\partial t} \tag{4}$$

as the total fluctuating pressure at the stagnation point. This is the result after the mean portion of the signal is electrically subtracted by physically engaging the averaging circuits in the Sanborn amplifier, setting the output voltage to zero using the position control, then disengaging the averaging circuit.

The output signal, which now represents only p_T', can be analyzed further by measuring its root mean square value. This is accomplished using a meter (Greibach Transquare Mo. 500) with a low frequency response flat to zero.

Mathematically, this is equivalent to squaring, taking the time average, and extracting the square root in that order. Squaring and meaning gives:

$$\overline{p_T'^2} = \rho^2 \overline{u_1}^2 \overline{u_1'^2} + 2\rho \bar{u}_1 \overline{u_1' p'} + \frac{1}{4}\rho^2 \overline{u_1'^4} - \frac{1}{4}\rho^2 \overline{u_1'^2}^2 + \overline{\rho u_1'^2 p'} + \overline{p'^2}$$

$$+ \rho R \overline{u_1'^2 \frac{\partial u_1'}{\partial t}} + R^2 \overline{\left(\frac{\partial u_1'}{\partial t} \right)^2} + 2R \overline{p' \frac{\partial u'}{\partial t}} \tag{5}$$

In order to assess the relative importance of each term, an order-of-magnitude analysis was performed assuming unity correlation coefficients for each correlation, a 25 per cent turbulence level, and a simple Bernoulli relationship between the fluctuating velocities and pressures. Assigning a value of 100 to the first and most important term on the right-hand side gives,

for the terms of Eq. 5 in order:

$$\overline{[p_T'^2]} = [100] + [25] + [1.56] - [1.56] + [3.1] + [1.56] + [0.2] + [\sim 0] + [0.2]$$

At lesser turbulence levels the first term is even more dominant. It is reasonable to neglect the last seven terms based simply on order-of-magnitude arguments. A similar analysis using the velocity potential of a sphere shows even less effect contributed by the time derivative of the velocity potential term.

It is known that the velocity-pressure correlation in the second term, rather than having a unity correlation coefficient, has a very small coefficient. For isotropic turbulent situations this correlation is zero. If this term is therefore also neglected and the square root is taken, the equation

$$\left(\overline{p'^2}\right)^{\frac{1}{2}} = \rho \overline{u_1} \left(\overline{u_1'^2}\right)^{\frac{1}{2}} \tag{6}$$

results. At higher intensities an estimated correction can be calculated, based upon the weight of the terms, and applied to the measurements.

In the above analysis the fluctuations in density are assumed to be controlled by the entrainment process at the toe of the jump. Correlations involving the density are therefore neglected.

The static pressures are measured by manometers. Symmetrical damping was applied by means of a pinch clamp on the plastic tubing to avoid any rectified effects due to fluctuating flow in the lines.

Since the primary energy was contained in a relatively narrow range around 1 or 2 Hz it was important that all the transducers and electronic equipment be direct coupled and have frequency characteristics flat to D.C. The static components of the signal corresponding to either the mean velocity or the mean pressure were measured and electrically "bucked out", leaving only the entire fluctuating portion.

The power spectra of the fluctuating bed pressures were determined by recording the signal at a slow tape speed and then scaling the frequencies into the range of the available analyzer by playing back the tape at a speed 64 times greater than the recorded speed.

The sample length was 64 minutes, which provided a one-minute playback time. Using this procedure, real time frequencies down to 0.5 Hz could be examined with a 0.172 Hz effective filter bandwidth. A 128 second effective averaging time was used.

The estimate of the signal density level was improved by widening the filters and suitably adjusting the levels as suggested originally by Morrow.[5] In essence two analyses were made, one to establish the spectrum detail and one to establish the power spectral density. A block diagram of the analyzing equipment is shown in Figure 5.

RESULTS

Hydraulic jumps are usually classified according to their incident Froude number:

$$Fr = \frac{V_1}{\sqrt{g\, d_1}} \tag{7}$$

where V_1 = the average inflowing velocity and g = acceleration due to gravity. In this study, jumps in the Froude number range between 3.69 and 11.6 were investigated. The results were generally similar, and for the purposes of this paper the Fr = 6.50 jump will be used as an example. The mean longitudinal pressure distribution on the bed will be utilized as a general indication of the jump profile.

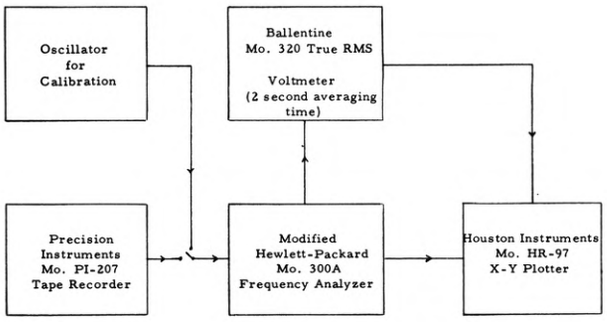

Figure 5. Scheme of the Power Spectrum Analyzing Equipment

The data of Figure 6 illustrate a map of equiconcentration contours of entrained air within the jump. With this information the fluid density was determined and the mean velocity profiles could be estimated from the manometer indication of the total head tube. The integration of the velocity profiles allowed the determination of the mean streamline map shown in Figure 7.

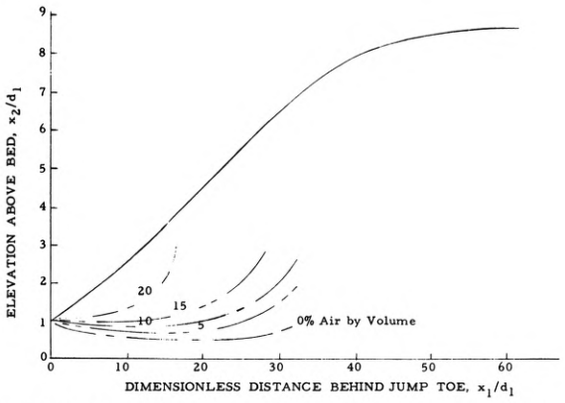

Figure 6. Equiconcentration Contours of Entrained Air, Fr = 6.5, d_1 = .095 ft., V_1 = 11.38 fps

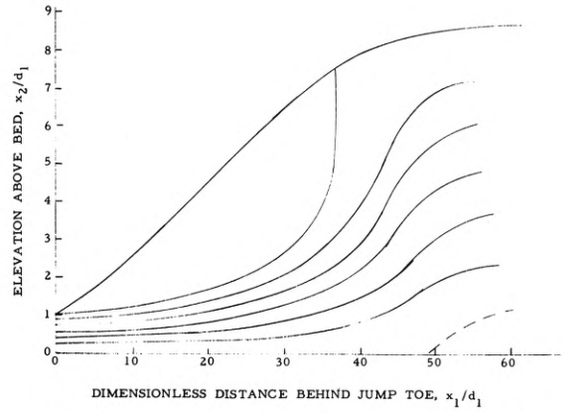

Figure 7. Mean Streamline Pattern, Fr = 6.5, d_1 = .095 ft., V_1 = 11.38 fps

The boundary of the surface roller is indicated by the surface streamline and the intersecting streamline. A separation zone on the bed just downstream of the surface roller is indicated by the dashed contour. The extent or size of the separation zone on the bed increased with increasing Froude number.

The longitudinal turbulent velocity profiles are shown in Figs. 8a and 8b for various distances downstream of the toe of the jump. The open symbols indicate the velocities obtained from Eq. 6. At low turbulence intensities Eq. 6 is accurate enough. At higher intensities corrections should be made involving higher order terms and correlations which begin to become important. The solid symbols are values corrected by estimating the values of the neglected higher order terms in Eq. 5.

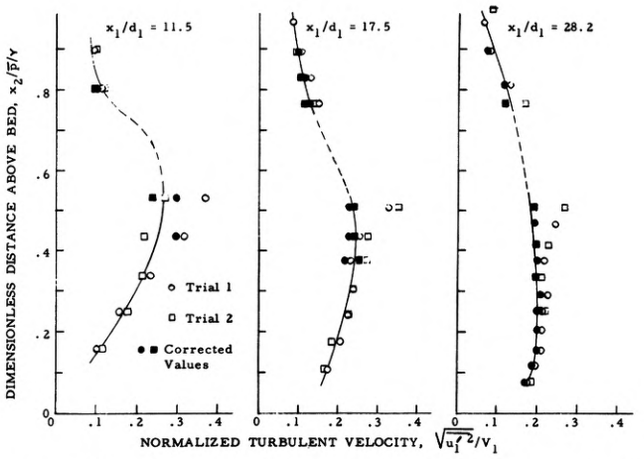

Figure 8A. Turbulence Velocity Profiles, Fr = 6.5, d_1 = .095 ft., V_1 = 11.38 fps

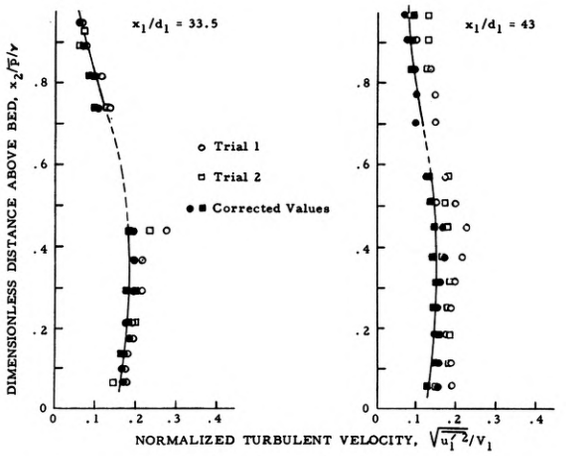

Figure 8B. Turbulence Velocity Profiles, Fr = 6.5, d_1 = .095 ft., V_1 = 11.38 fps

The dashed portions of the curves indicate the region where flow reversal takes place and the turbulence intensity is greater than 100 per cent. Under these conditions no meaningful reduction of the fluctuating stagnation pressure data was possible and the data were discarded. The solid portions of the curve were simply linked up with the dashed lines. The magnitude of the turbulence was normalized with the incoming average mean velocity, V_1.

These data compare very well with those obtained by Rouse, et al.[1] in an air model of a hydraulic jump until about the end of the surface roller, or approximately x_1/d_1 = 35 to 40 for Fr = 6.5. After that point the turbulence levels in the current study remained up to four times higher than the air model results.

In a recent study of turbulence downstream of a hydraulic jump Resch and Leuthheusser[6] show that such differences are caused by the velocity profile of the inflowing supercritical sheet. A flat constant inflowing velocity profile produced residual turbulence levels similar to the air model results and a developed profile produced residual turbulence approximately four times greater. The findings of the present study where the inflowing profile was developed clearly agree with these results.

One of the primary objectives of the research was to establish means by which the fluctuating pressure measurements obtained on a hydraulic model could be used to make prototype predictions.

If the gravitational force and a length scale are considered of primary importance, dimensional arguments lead to expressing the dimensionless power density as:

$$\frac{n^2 g^{\frac{1}{2}}}{\overline{p'^2}\,(d_1)^{\frac{1}{2}}}$$

and the dimensionless frequency as:

$$\frac{f\,(d_1)^{\frac{1}{2}}}{g^{\frac{1}{2}}}$$

The total root mean square fluctuating pressure, according to the same argument, can be made dimensionless either with the characteristic length and the specific weight of water, γd_1, or with the incoming velocity head, $\alpha\gamma V_1^2/2g$. In this connection γ is the specific weight of the water and α is the usual energy coefficient calculated from the incoming velocity profile, defined as:

$$\alpha = \left(\int_0^{d_1} \overline{u_1}^3 \, dx_2 \right) / V_1^3 d_1 \qquad (8)$$

The experimental data taken in the 20 inch and 9 foot channels shown in Figure 9 indicate that satisfactory agreement can be achieved in scaling the total fluctuating pressure using these arguments. The neglect of the energy coefficient, α, resulted in much greater discrepancies in all jumps tested, while its inclusion generally improved the scale comparisons a great deal.

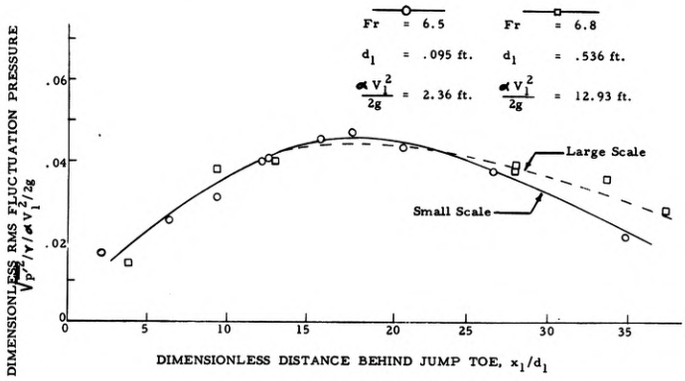

Figure 9. Effect of Scale on Bed RMS Fluctuation Pressure, Fr ~ 6.5

Comparisons of Figures 10 and 11 indicate that general agreement of the power spectra was obtained. The data of Figure 10 for the flow in the smaller channel should be considered of higher quality than the data of Figure 11 for the large-scale tests. Experimental difficulties encountered with the large flows restricted somewhat the accuracy with which the measurements could be made. The mode dimensionless frequency and dimensionless power density for the small- and large-scale tests generally correspond.

The power spectra were taken at various positions on the channel beds and indicate a changing shape as the flow develops. The energy content is shifted generally to lower frequencies as the observation point is moved downstream. The spectra show a maximum or a mode in the reduced frequency range of 0.1 to 0.2 and fall off in both directions on either side. At very low frequencies the spectra again increase. It is believed, however, that

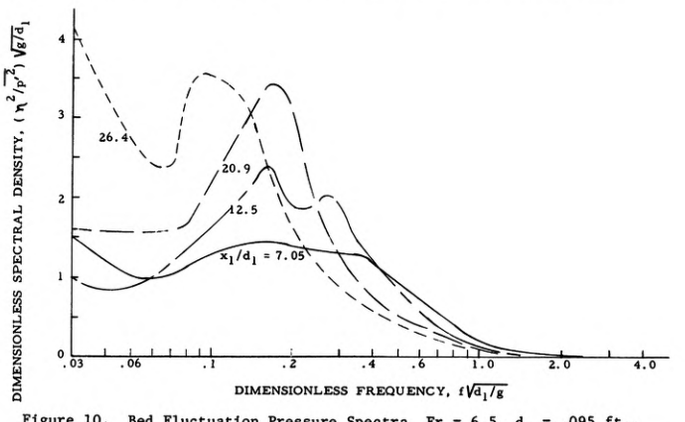

Figure 10. Bed Fluctuation Pressure Spectra, Fr = 6.5, d_1 = .095 ft., V_1 = 11.38 fps

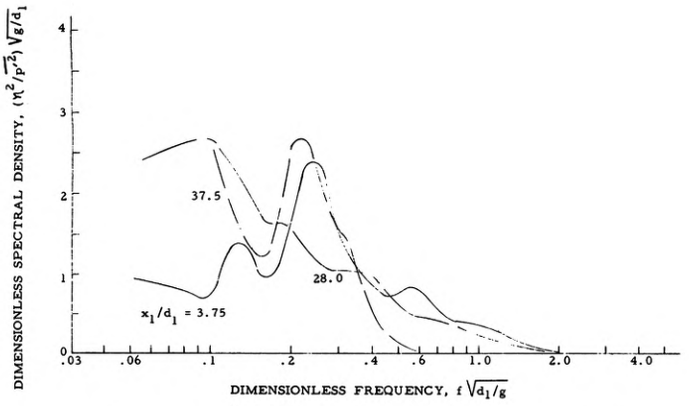

Figure 11. Bed Fluctuation Pressure Spectra, Fr = 6.8, d_1 = .536 ft.

this may be caused either by the slight overall unsteadiness of the flow (the jump moving slightly forward and back in the channel) or by the inability to maintain the frequency analyzer in proper adjustment at the very low end of its range of operation.

CONCLUSIONS

1. The mean streamline pattern clearly reveals the outline of the surface roller. This pattern also shows the boundary layer separation and a boundary roller just downstream of the surface roller.
2. The longitudinal component of the turbulent velocity compared very favorably with the values measured by Rouse, et al.[1] in the air model to approximately the end of the roller.
3. The turbulence levels in the flow immediately downstream of the jumps were of the order of 4 times higher than those indicated by the air model.
4. The study by Resch and Leutheusser[6] explains the difference in downstream turbulence level according to the significant effect of the inflowing velocity profile. The lower downstream turbulence levels result from a potential type inflow, while the higher levels result from a developed boundary layer inflow profile.
5. The maximum measured longitudinal turbulence was approximately 30 per cent of the inflowing mean velocity. This value occurred near the toe of the jump.
6. The maximum value of the rms pressure fluctuation on the bed occurred about midway under the surface roller and was approximately 5 per cent of the inflowing specific kinetic energy, $\alpha V_1^2/2g$. The macropressure fluctuations on the bed die out near the end of the surface roller.
7. The energy in the power spectrum is generally concentrated in the dimensionless range, $0.1 < f\sqrt{d_1/g} < 1.0$. The shift in energy is toward the lower frequencies as the observation point is moved downstream under the jump.
8. The dimensionless spectral density, $(\eta^2/\overline{p'^2})(g/d_1)^{1/2}$, generally ranged between 2.0 and 4.0 in the region of the mode.
9. The scaling relationship between the small- and large-scale tests, based on Froude laws for the dimensionless rms fluctuating pressure, was quite good provided the energy factor, α, of the incoming flow was included. This is additional evidence regarding the importance of the nature of the inflowing stream.
10. General agreement was achieved in the scaling of the power spectra. The physical difficulties encountered in the large-scale tests limited the accuracy of the measurements to such a degree that they were not useful for very precise scaling comparisons.

ACKNOWLEDGMENTS

The study was conducted under a grant from the National Science Foundation.

SYMBOLS

d_1	water depth just upstream of the jump
f	frequency
Fr	incident Froude number
F(t)	function of time
g	acceleration due to gravity
$\overline{P_T}$	mean stagnation pressure
$\overline{p}$	pressure
p'	fluctuating component of pressure
p'_T	fluctuating component of stagnation pressure
R	radius of turbulence probe
t	time
$\overline{u_i}$	mean velocities i = direction of the vector: 1 indicates longitudinal direction, 2 indicates vertical direction
u_i'	turbulent component of velocity
V_1	mean inflowing velocity
x	distance
x_s	distance between the point source and the stagnation point
α	energy factor
η^2	fluctuation pressure power density
ρ	fluid density
ϕ	velocity potential

REFERENCES

1. Rouse, H., Siao, T. T., and Nagaratnum, S., "Turbulence Characteristics of the Hydraulic Jump", Trans. ASCE, 124, 926-966 (1959).
2. Gardner, S., "On Surface Pressure Fluctuations Produced by Boundary Layer Turbulence", Acustica, 16, 67-74 (1965).
3. Lamb, O. P. and Killen, J. M., An Electrical Method for Measuring Air Concentration in Flowing Air-Water Mixtures, Technical Paper No. 2-B, St. Anthony Falls Hydraulic Laboratory, University of Minnesota, March 1950.
4. Arndt, R. E. A. and Ippen, A. T., "Turbulence Measurements in Liquids Using an Improved Total Pressure Probe", Journal of Hydraulic Research, Vol. 8, No. 2, 1970.
5. Morrow, C. T., "Averaging Time and Data Reduction Time for Random Vibration Spectra", J. Acoust. Soc. Amer., 30, 572-578 (1958).
6. Resch, F. J. and Leutheusser, H. J., "Mesures de Turbulence Dans Le Ressant Hydraulique", La Houille Blanche, No. 1, 1971.

DISCUSSION

J. WAY (Illinois Institute of Technology): What was the averaging time that you used in your averaging circuit that you then used to bias out your steady or your DC values?

SCHIEBE: The time constant for the low pass filter was of the order of 4 seconds.

WAY: Did you attempt any visualization at all within the jump to corroborate the stream lines?

SCHIEBE: Well, you can't see through the bubbly mess, but what we did do was to look at the separated zone on the bed. We put dye in there. And there is

a separated zone there on the average. Sometimes our dye was swept away and sometimes it stayed and sometimes we could see reversing flow. The flows inside that separated zone were too small to measure with a total head tube.

WAY: What kind of transducers did you use along the bed?

SCHIEBE: We used flush mounted Statham and Consolidated strain element transducers. They are a half inch in diameter, which I don't think causes any problem with the frequencies we were looking at.

H. M. NAGIB (Illinois Institute of Technology): You showed two spectra, one on the large scale and one on the small scale. And you showed some peaks in there. Do you have any remarks on what is causing this peak in the spectra? It appears that there is something regular that is happening at this frequency. Could it be your roller jumping over the separated region?

SCHIEBE: One of the other things that I did which I didn't mention is to look at the streamline pattern roller and calculate the time for fictitious fluid particles to go around. As I expected, I found a vortex there. And this frequency turned out to be much lower, converting that to frequency, than the mode we observed.

T. HOULIHAN (Naval Post-Graduate School): What was the ratio of the magnitudes of the remaining AC signal to the total signal after the DC was subtracted out?

SCHIEBE: In the case of the fluctuating bed pressure at its maximum value, the fluctuating signal was 20 per cent of the static pressure. This ratio, of course, varies with position under the jump.